Journal Title
XX(X):1–18
©The Author(s) 2017
Reprints and permission:
sagepub.co.uk/journalsPermissions.nav
DOI: 10.1177/ToBeAssigned
www.sagepub.com/
SAGE

A robust walking controller based on online step location and duration optimization for bipedal locomotion

Majid Khadiv[1,2], Alexander Herzog[1], S. Ali A. Moosavian[2] and Ludovic Righetti[1]

Abstract

Step adjustment for humanoid robots has been shown to improve gait robustness, while timing adjustment is often neglected in control strategies. In this paper, a new walking controller is proposed that combines both step location and timing adjustment for generating robust gaits. In this approach, step location and timing are decided, based on the Divergent Component of Motion (DCM) measurement. We define the "DCM offset" as the offset between the DCM and landing location of the swing foot at landing time, and employ it to split state space into viable/non-viable parts. Constructing our walking controller based on the DCM offset, we can exploit the whole capability of a biped robot in terms of stepping to recover from disturbances. The proposed approach is comprised of two stages. In the first stage, the nominal step location and step duration for the next step(s) are decided. In this stage, the main goal is to schedule the gait variables far from constraint boundaries for a desired walking velocity. The second stage adapts at each control cycle the landing position and time of the swing foot. By using the DCM offset and a change of variable for the step timing, we can formulate the second stage of our controller as a small sized quadratic program without the need to preview several steps ahead. The swing foot trajectory is also re-planned at each control cycle to realize adapted landing properties. To map the adapted gait variables to the full robot, a hierarchical inverse dynamics is employed. Interestingly, our approach does not require precise control of the center of pressure and can also be used on robots with passive ankles or point feet. Simulation experiments show a significant improvement in robustness to various types of external disturbances, such as pushes and slippage, compared to state of the art preview controllers where step timing is not adjusted. In particular, we demonstrate robust walking behavior for a simulated robot with passive ankles.

Keywords

bipedal locomotion, robust walking, step timing adjustment

arXiv:1704.01271v1 [cs.RO] 5 Apr 2017

1 Introduction

* Due to the unilateral nature of feet-ground interaction, legged robots are prone to fall down during their maneuvers. Since falling down can be costly because of hardware damages, the most important factor in designing walking controllers is to minimize the possibility of falling down even in case of strong perturbations. In this regard, a controller should decide where to put the feet (step adjustment), when to make a step (step timing adaptation), and how to move the body to keep the robot balance (Center of Pressure (CoP) modulation). Because of physical constraints on each of these tools for preserving the robot balance and steering its motion, employing an optimal combination of these tools consistent with hardware and environment constraints is a necessity.

Traditional walking controllers used predefined step locations and timing to steer the robot motion. They relied on a predefined feasible Zero Moment Point (ZMP) trajectory Kajita et al. (2003), or CoP modulation Wieber (2006) to steer the robot Center of Mass (CoM) and keep balance. These controllers employ available interaction forces to control the CoM in a Linear Inverted Pendulum Model (LIPM) setting. Although CoP modulation has the advantage of high control bandwidth, it is limited to the size of the foot. Furthermore, manipulating the CoP with sufficient precision requires actuators located directly at the ankle. Hence, CoP modulation becomes difficult without ankle actuation (e.g. the Sarcos humanoid robot Athena shown in Figure 6), because it requires acceleration of the upper body joints. Moreover, CoP modulation is impossible (assuming instantaneous double support phase) for robots with point contact feet (e.g. ATRIAS Hubicki et al. (2016)).

Taking a step can be chosen from a less restrictive range of possibilities (the reachable area for the swing foot) compared to CoP modulation (support polygon). Moreover, it can be used for controlling robots with different foot geometries without any restriction. Hence, a controller which just relies on step adjustment for keeping the robot balance and steering

[1]Autonomous Motion Department, Max-Planck Institute for Intelligent Systems, Germany
[2]Department of Mechanical Engineering, K. N. Toosi University of Technology, Tehran, Iran

Corresponding author:
Majid Khadiv, Autonomous Motion Department, MPI for Intelligent systems, Paul-Ehrlich-Str. 15, Tübingen, Baden-Württemberg 72076, Germany.
Email: majid.khadiv@tuebingen.mpg.de , mkhadiv@mail.kntu.ac.ir

*Part of the material presented in this paper has been presented at the 2016 IEEE/RAS International Conference on Humanoid Robots (Humanoids), Khadiv et al. (2016a)

its motion can be employed for robots with different foot geometries and ankle actuations. However, step adjustment can be done on a higher frequency (each step) compared to CoP modulation (each control cycle). The frequency of stepping has been considered fixed in most previous works Kajita et al. (2003); Wieber (2006); Herdt et al. (2010a); Pratt et al. (2012); Englsberger et al. (2015), but can be adapted through step timing adjustment to enhance robustness in gaits. As a result, algorithms need to be developed that can optimize both step location and timing, which is a general approach for controlling robots with different foot geometry and ankle actuation.

1.1 Related work

Generating walking patterns exploiting the whole dynamics of humanoid robots is a general approach which can deal with multi-contact interaction with environment and walking on different surfaces Tassa et al. (2012); Lengagne et al. (2013); Kudruss et al. (2015); Khadiv et al. (2015); Herzog et al. (2015, 2016b); Carpentier et al. (2016). However solving a high dimensional nonlinear optimization demands high computation burden. Furthermore, due to the non-convexity of the problem, convergence to the global minimum is not guaranteed and the methods can be very sensitive to an initial guess. Although convex models of the momentum dynamics have been proposed Ponton et al. (2016), simplified linear models that capture the task relevant dynamics to a set of linear equations are useful for generating walking patterns in real-time.

The Linear Inverted Pendulum Model (LIPM) Kajita et al. (2001), has been very successfully used for the design of walking controllers for complex biped robots. Since there exists an analytical solution for this model, analytical methods for walking pattern generation have been widely used. In traditional analytical approaches, the position and velocity of the CoM were employed to generate a trajectory for the CoM consistent with a predefined ZMP trajectory Harada et al. (2006); Morisawa et al. (2006, 2007); Buschmann et al. (2007). By constraining the position and velocity of the CoM during motion planning, both divergent and convergent parts of the LIPM dynamics are constrained. In contrast, Takenaka et al. (2009) constrained only the divergent part of the CoM dynamics to generate a trajectory for the Divergent Component of Motion (DCM) based on predefined footprints (ZMP trajectory). Before Takenaka et al. (2009), the divergent part of the LIPM dynamics had been used by Hof (2008) to explain human walking properties under the name of extrapolated Center of Mass (XCoM). This concept was originally developed in Pratt et al. (2006) under the name of Capture Point (CP), the point on which the robot should step to come to rest.

In these analytical methods for walking pattern generation, the trajectories are updated based on high-level commands for changing the walking characteristics, i. e. walking velocity, step length, etc. However, there is no feedback loop to adapt the generated patterns in the presence of disturbances and uncertainties. To circumvent this, Englsberger et al. (2015) proposed a feedback law to track a DCM trajectory that is generated using the analytical solution of the LIPM. Although this controller can react to the disturbances very fast, perfect DCM tracking needs unconstrained manipulation of the CoP.

All of the motion planners based on analytical methods can be seen as variants of the same Model Predictive Control (MPC) scheme Wieber et al. (2016). One of the pioneer works that related the walking pattern generation for biped robots through an optimal control framework was done by Kajita et al. (2003). They proposed preview control of the ZMP to generate a CoM trajectory based on a predefined ZMP trajectory. One of the promising advantages of relating the problem in this framework is that the feedback from states of the system can be used to recompute and adapt the motion online. Wieber (2006) improved the performance of this approach in the presence of relatively severe pushes, by constraining the motion of the ZMP inside the support polygon rather than predefining a trajectory for it. As a result, in this trajectory free MPC scheme, motion of the ZMP and the CoM are recomputed at each control cycle for a preview period (but evaluated just for the next control cycle) respecting the feasibility constraints. In these approaches a preview over several steps is considered for gait planning, but fixed step location and timing are assumed for this preview period.

Manipulating the CoP/ZMP for controlling the DCM or the CoM has different restrictions for robots with different structures. For instance, for robots with point contact feet Hubicki et al. (2016) (assuming instantaneous double support phase), it is not possible to modulate the CoP, while for robots with passive ankles Khadiv et al. (2016b) the CoP cannot be manipulated directly by the ankle joints torques. In fact, changing the CoP location to control the DCM or CoM motion is limited to the robot structure, and in the best case can only be controlled directly inside the support polygon, using a limited amount of ankle torque. Contrary to the CoP manipulation for controlling the DCM or the CoM, step adjustment is a more significant tool for stabilizing biped robots. The reason is that the next step location can be selected in a relatively large area compared to the support polygon. As a result, step adaptation algorithms using analytical methods Englsberger et al. (2013, 2015); Khadiv et al. (2016b) as well as optimization approaches Diedam et al. (2008); Herdt et al. (2010a,b); Faraji et al. (2014a,b); Feng et al. (2016) have been suggested to make walking patterns more robust against disturbances. However, in all these methods the step timing is never adapted. The reason is that in order to keep the problem convex in a previewed number of steps, optimization based stepping pattern generators typically assume fixed step duration.

Compared to the CoP manipulation which is carried out at each control cycle, step adjustment is performed on a larger timing scale (each step time). Feng (2016) showed that using a combination of step location and timing adaptation increases significantly the basin of attraction for bipedal locomotion. Missura and Behnke (2013) proposed an analytical method for computing nominal gait variables for a desired walking velocity, and an algorithm for adapting both step location and timing based on heuristics. Castano et al. (2016) proposed an analytical method for step timing and foot placement adaptation based on the CoM state feedback, with a priority given to the sagittal gait. Griffin et al. (2017) modified the analytical approach in Englsberger

et al. (2015) by adjusting both step location and timing. They used step location and timing adjustment using heuristics to compensate for the DCM (or Instantaneous Capture Point (ICP)) tracking error. Apart from adjusting step timing to robustify gaits against disturbances, Park et al. (2006); Khadiv et al. (2017) adapted the single support duration to negotiate soon or late landing of the swing foot using contact detection.

Besides the proposed analytical methods, some works tried to use the step duration as an optimization variable Aftab et al. (2012); Kryczka et al. (2015), however they resulted in a nonlinear optimization problem which is computationally expensive and also convergence to the global minimum is not guaranteed. Maximo et al. (2016) proposed an extension of the gait planning approach in Herdt et al. (2010a) to adjust step duration. They related the problem through a Mixed-Integer Quadratic Program (MIQP) which has combinatorial complexity. Furthermore, Caron and Pham (2016); Caron and Kheddar (2017) used timing adaptation to limit the acceleration of the swing foot, during walking on uneven terrains.

In all of these analytical and optimization-based methods for walking pattern generation, viability Wieber (2002, 2008) or capturability Pratt et al. (2006); Koolen et al. (2012) of the motion is guaranteed by limiting an integral of states of the system in a previewed period Wieber et al. (2016). This can be realized by setting a terminal condition on the states in a previewed number of steps as a sufficient condition of viability Takenaka et al. (2009); Englsberger et al. (2015), or by minimizing other forms of viability Kajita et al. (2003); Wieber (2006); Herdt et al. (2010a). As a result, a previewed number of steps is considered to guarantee that the motion of the CoM/DCM does not diverge.

1.2 Proposed approach

In this paper, we propose a stepping schedule generator for robust walking. Our algorithm does not rely on CoP modulation, which makes it suitable for robots with various endeffector geometry, i. e. actuated or unactuated ankles or even point feet. We compute foot step locations online that steer the CoM in a desired way which is especially suited for robots with little or no ankle actuation. Different to common LIPM walking pattern generators, we not only optimize over foot step locations, but also over stepping frequency enhancing robustness of walking. In fact, our walking controller adapts automatically both the swing foot landing location and time. Since the system dynamics is nonlinear with respect to timing, we propose a change of variable which renders the problem linear and allows us to solve it with a small sized convex Quadratic Program (QP).

Rather than considering several steps ahead to guarantee viablity of the motion, our optimizer tries to realize a desired offset between the DCM and the swing foot landing location (we name this value "DCM offset") to prevent the DCM to diverge. As a result, our optimizer is an efficient small sized QP that adapts both swing foot landing location and timing at each control cycle, using feedback from current state of the robot. We show that using the DCM offset, we can split state space to viable/non-viable parts. Hence, constructing the problem in terms of DCM offset, our proposed controller recovers the robot from disturbances if the current state is viable. It should be noted that the idea of DCM offset has been motivated by Hof (2008), where it was shown that this offset is the key factor to address human walking properties.

We generate Cartesian swing leg trajectories and control them inside of a hierarchical inverse dynamics on the whole-body Herzog et al. (2016a). In this framework, we obtain the torque commands for a torque-controlled biped robot, consistent with a hierarchy of tasks and constraints in real-time. Since our gait optimizer does not rely on CoP manipulation for controlling the DCM, it is not necessary that the CoP is controllable. This means that the generated gaits can be very aggressive such that the stance foot rotates around the edges (in a way consistent with the robot dynamics). This also means that our controller can also handle slippage of the stance foot although the CoP is not controllable anymore.

First, to demonstrate the robustness of our method, we conduct simulations using a LIP model of the robot in the presence of different disturbances. Comparison with state of the art preview controllers shows a significant robustness improvement when timing adaptation is added to step adjustment. Then, we present experimental results on a simulated humanoid robot with passive ankles and prosthetic feet. The conducted simulation experiments on different scenarios show robust walking performance in the presence of various pushes on the pelvis (push recovery) and stance foot (slippage recovery).

This paper is an extension of our preliminary work Khadiv et al. (2016a), where we proposed an optimization problem based on the DCM offset concept to control step location and timing, and demonstrated its effectiveness using simulation of the LIPM. In this paper, we use the DCM offset to split state space into viable/nonviable parts. This allows us to show that our control problem in terms of the DCM offset will always find a feasible solution as long as the current robot state is viable. We employ the hierarchical inverse dynamics controller proposed in Herzog et al. (2016a) to map the generated policies to the full robot. Moreover, we conduct various simulation scenarios on a full humanoid and show the capability of our controller in recovering from slippage in addition to strong external pushes.

The rest of this paper is structured as follows: Section 2 describes the fundamentals and viablity considerations. In Section 3, the proposed optimization-based walking controller for adjusting step location and timing is described. Section 4 deals with generating online swing foot trajectory to realize the adapted gait variables. In Section 5, the whole body controller and the set of tasks and constraints are addressed. In Section 6, simulation results obtained from the LIP model of a humanoid robot, as well as comparison of the proposed walking controller with state of the art is presented. Section 7 is dedicated to full humanoid simulations on various scenarios. Section 8 discusses the obtained results. Finally, Section 9 concludes the findings.

2 Fundamentals

The LIPM constrains motion of the CoM on a plane (horizontal plane for walking on a flat surface), by using a telescopic massless link connecting the CoP to the CoM Kajita et al. (2001). The dynamics of this system may be

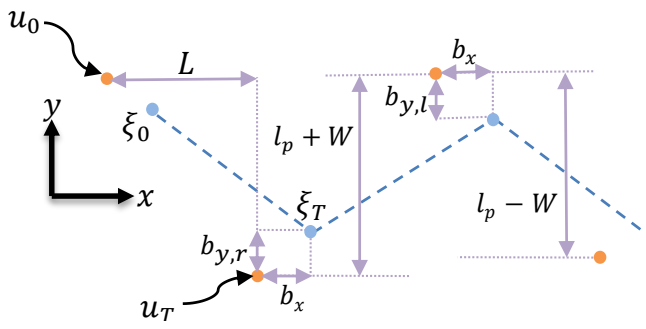

Figure 1. A schematic view of the walking pattern showing the footprints, the DCM, and the DCM offset

formulated as:

$$\ddot{x} = \omega_0^2(x - u_0) \tag{1}$$

in which x is a 2-D vector containing CoM horizontal components (the vertical component has a fixed value z_0), and u_0 is the CoP vector ($u_0 = [CoP_x, CoP_y]^T$). For a robot with point contact feet, u_0 stands for the contact point. Furthermore, ω_0 is the natural frequency of the pendulum ($\omega_0 = \sqrt{g/z_0}$, where g is the gravity constant, and z_0 is the CoM height).

By considering CoM (x) and DCM ($\xi = x + \dot{x}/\omega_0$) as the state variables, the LIPM dynamics in the state space form may be specified as:

$$\dot{x} = \omega_0(\xi - x) \tag{2a}$$

$$\dot{\xi} = \omega_0(\xi - u_0) \tag{2b}$$

Equation (2) decomposes the LIPM dynamics into its stable and unstable parts, where the CoM converges to the DCM (2a) and the DCM is pushed away by the CoP (2b). Hence, in order to have a stable walking pattern, it is enough to constrain the DCM motion during walking, without restricting the stable part of the system. Based on (2b), one possibility for limiting the DCM motion is to constrain the DCM at the end of a specified time $\xi(T)$ Englsberger et al. (2015). In fact in this case, a terminal condition (captured state) is set at the end of a previewed number of steps (predefined), and using a recursive procedure the DCM at the end of the current step is computed. Then, the differential equation is solved as a final value problem and by having a limited value at the end of a specified time, the DCM trajectory converges. However, further inspection on (2b) reveals that this is not the only way to keep the DCM from diverging. In fact, a legged robot can instantaneously change its CoP location u_0 at a specified time by taking a step Pratt et al. (2006); Koolen et al. (2012) in order to limit the DCM motion. Using this concept, it is not required to choose predefined step locations for a previewed number of steps. Hence, we can constrain and steer the DCM motion, just by choosing appropriate location and time for taking the next step.

2.1 DCM offset

By solving (2b) as an initial value problem, the DCM motion based on the natural dynamics of the LIPM can be obtained:

$$\xi(t) = (\xi_0 - u_0)e^{\omega_0 t} + u_0 \tag{3}$$

The DCM at the end of a step is obtained by substituting the step duration T in (3):

$$\xi_T = (\xi_0 - u_0)e^{\omega_0 T} + u_0 \tag{4}$$

Now, we define the DCM offset as:

$$b = \xi_T - u_T \tag{5}$$

where u_T is the next step location and ξ_T is the DCM at the end of the step (Figure 1). By solving (2b) as a final value problem, we can write the LIPM solution in terms of the next footprint location, the step duration, and the DCM offset:

$$u_T = (\xi_{cur} - u_0)e^{\omega_0(T-t)} + u_0 - b \quad , \quad 0 \le t \le T \tag{6}$$

in which ξ_{cur} is the current DCM.

The DCM offset b has a crucial role in our walking controller. Realizing a DCM offset less than a maximum value at the end of a step guarantees viability of the walking system in the next step. The maximum value for the DCM offset is obtained using the kinematic and dynamic constraints of a walking system and will be discussed in the next subsection. Furthermore, by achieving a desired DCM offset at the end of a step, we make sure that the CoM travels a desired distance during a specified time in the next step (without perturbation) which realizes a desired average velocity during T. Using (4) and (5), the desired DCM offset in sagittal/lateral direction for having a desired step length(L)/step width (W) during a desired step time (T) is computed (The derivation procedure is given in Appendix B):

$$b_x = \frac{L}{e^{\omega_0 T} - 1} \tag{7a}$$

$$b_y = (-1)^n \frac{l_p}{1 + e^{\omega_0 T}} - \frac{W}{1 - e^{\omega_0 T}} \tag{7b}$$

in which l_p is the width of the robot pelvis (the default step width) and n is the index for distinguishing the left and right foot ($n = 1$ when the right foot is stance, and $n = 2$ when the left foot is stance). It should be noted that W describes the deviation of the step width with respect to the default step width l_p. In fact, this value shows how much the robot moves laterally, so we name it "step width" (Figure 1).

2.2 DCM offset and viability

For bipedal walking, we are generally interested in finding a part of state space from which the robot is able to avoid falling. Based on the viability theory Aubin (1991); Aubin and Cellina (2012), this subset of state space is defined as the viable region Wieber (2002, 2008). Since computing this area is generally intractable Wieber (2002, 2008), a sufficient condition for viability (based on a preview of several steps) is typically adopted for bipedal walking pattern generation Wieber et al. (2016). However, using the idea of DCM offset, we can compute the exact viable part of state space based on the LIPM abstraction of a biped, just by looking at the end of the current step. This means that the DCM offset enables us to relate the problem of walking pattern generation through a small sized optimization problem (next section). In this subsection, we demonstrate the relation between the DCM offset and viability. We limit our analysis to the

sagittal direction for forward walking, while the procedure for backward walking is similar. The corresponding analysis for the lateral direction is given in Appendix C.

To realize a forward walking task with step length L and step duration T, the desired DCM offset and the constraints can be specified as:

$$\begin{aligned} b_x &= \frac{L}{e^{\omega_0 T} - 1} \\ L &\leq L_{max} \\ T &\geq T_{min} \end{aligned} \tag{8}$$

where L_{max} and T_{min} are the maximum step length and minimum step duration, respectively. Using the contraints, the maximum allowable DCM offset can be computed:

$$b_{x,max} = \frac{L_{max}}{e^{\omega_0 T_{min}} - 1} \tag{9}$$

To show that this value exactly splits the state space into the viable and non-viable areas, we consider two cases. In the first case, we consider a DCM offset larger than this value and show that all possible evolutions starting from this state cause divergence/fall. In the second case, we show that for DCM offsets smaller than this value, there exists at least one evolution that keeps the DCM from diverging. As a result, the value in (9) specifies an exact bound for viable/non-viable states.

Case I: The DCM offset is larger than $b_{x,max}$ at the start of a step:

$$\xi_{x,0} - u_{x,0} = \frac{L_{max}}{e^{\omega_0 T_{min}} - 1} + \epsilon \tag{10}$$

we can compute the DCM offset at the end of the step using (4), (5) and (10):

$$b_x = (\frac{L_{max}}{e^{\omega_0 T_{min}} - 1} + \epsilon) e^{\omega_0 T} - (u_{x,T} - u_{x,0}) \tag{11}$$

in which ϵ is an arbitrary positive number. Substituting $u_{x,T} - u_{x,0} = L_{max}$ and $T = T_{min}$, the minimum realizable value of b_x in (11) is obtained as:

$$b_x = \frac{L_{max}}{e^{\omega_0 T_{min}} - 1} + \epsilon\, e^{\omega_0 T_{min}} \tag{12}$$

Comparing (10) and (12), it is clear that the minimum realizable DCM offset at the end of the step is increased by a factor $e^{\omega_0 T_{min}}$ times ϵ. In a sequence of steps, this constitutes a geometric series with the common ratio of $e^{\omega_0 T_{min}}$ which diverges as time passes. As a result, all realizable evolutions starting from a DCM offset more than (9) cause divergence/fall.

Case II: The DCM offset is smaller than $b_{x,max}$ at the start of a step:

$$\xi_{x,0} - u_{x,0} \leq \frac{L_{max}}{e^{\omega_0 T_{min}} - 1} \tag{13}$$

Using (4), (5), and (13), the following constraint on the DCM offset at the end of a step is computed:

$$b_x \leq (\frac{L_{max}}{e^{\omega_0 T_{min}} - 1}) e^{\omega_0 T} - (u_T - u_0) \tag{14}$$

In this case we aim at showing that from this state, there exists at least one evolution that does not lead to a fall/divergence. If we consider $u_T - u_0 = L_{max}$ and $T = T_{min}$, the following inequality is derived:

$$b_x \leq \frac{L_{max}}{e^{\omega_0 T_{min}} - 1} \tag{15}$$

Comparing (13) and (15), it can be concluded that starting from a state in (13), there exists at least one evolution that causes a DCM offset inside the same area at the end of the step. As a result, this state is viable.

Based on these two cases, we can conclude that the value in (9) exactly distinguishes viable states from non-viable states for the LIPM abstraction of a biped. The interesting point is that this value is the same as the ∞-step capture basin bound for the LIPM with point contact in Koolen et al. (2012). The difference is that ∞-step capturability just shows how capturable the robot in the current state is, and cannot be employed as a control variable. However, the DCM offset can be used as a decision variable to realize a desired motion as well as to exploit the whole capability of a biped robot to recover from external disturbances. The DCM offset has the key role in our walking controller which will be formulated in the next section.

3 Stepping controller

As it is illustrated in Figure 2, our proposed stepping controller is comprised of two stages. The first stage generates nominal values for the step location, step duration, and the DCM offset for a desired walking velocity. Given the nominal values, the second stage generates the desired location and time for the swing foot landing at each control cycle, based on DCM measurement. Then, the outputs of this stage are exploited for generating swing foot trajectory (Section 4). The generated trajectories are then fed to the whole body controller to generate desired torques for the robot joints (Section 5).

3.1 First stage: specifying nominal values

In the first stage of our method, we propose a procedure to find the gait variables consistent with a desired walking velocity, rather than predefining these variables. In fact, in this stage we aim at finding a desired set of step length and width as well as step duration that satisfies the robot and environment constraints. Hence, the problem is to find the nominal step length L_{nom}, step width W_{nom}, and step duration T_{nom}, subject to kinematic and dynamic constraints:

$$\begin{aligned} v_x &= \frac{L_{nom}}{T_{nom}} \\ v_y &= \frac{W_{nom}}{T_{nom}} \\ L_{min} &\leq L_{nom} \leq L_{max} \\ W_{min} &\leq W_{nom} \leq W_{max} \\ T_{min} &\leq T_{nom} \leq T_{max} \end{aligned} \tag{16}$$

in which v_x and v_y are the desired average walking velocities in sagittal and lateral directions, respectively. The max and min indices show the bounds on the gait variables. It should

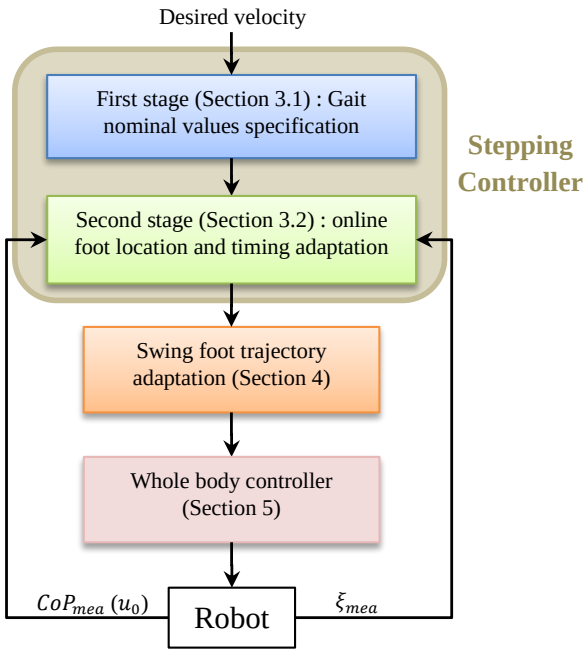
Desired velocity
First stage (Section 3.1) : Gait nominal values specification
Second stage (Section 3.2) : online foot location and timing adaptation
Stepping Controller
Swing foot trajectory adaptation (Section 4)
Whole body controller (Section 5)
$CoP_{mea}\,(u_0)$
Robot
ξ_{mea}

Figure 2. Block diagram of the proposed method. In the first stage, the nominal values which are the step length and step duration are decided based on a desired velocity and consistent with constraints. In the second stage, the location and landing time of the swing foot are adapted through a small sized QP optimization, using DCM measurement. To realize the adapted step length and step timing, the swing foot trajectory is regenerated at each control cycle. Finally, the generated trajectories are fed to the whole body controller to generate desired torques for the robot joints.

be noted that the inequality constraints on step location are a combination of the robot (limited step length and width) and environment (limited area for stepping) limitations. Besides, there is a constraint on the minimum step timing which limits the acceleration of the swing foot, while the constraint on the maximum step timing is to limit very slow stepping in our gait schedule.

Various performance criteria can be considered to find the best step length and width and step duration for a desired walking velocity. Though some studies have been carried out to address this for human walking Kuo et al. (2005); Kuo (2001), it seems more practical to consider some other criteria for biped robots walking with different limitations compared to human. For instance, one possibility is to minimize fluctuations on the instantaneous CoM velocity in order to have a smooth walking pattern. In this paper, we chose nominal step length and width according to a robustness criteria, where we maximize distance to their bounds. Selecting the variables far from the boundaries yields more versatility to adapt them in real-time (second stage). Combining the equality and inequality constraints of (16) yields:

$$\begin{aligned} B_l^1 = \frac{L_{min}}{v_x} \leq T_{nom} \leq \frac{L_{max}}{v_x} = B_u^1 \\ B_l^2 = \frac{W_{min}}{v_y} \leq T_{nom} \leq \frac{W_{max}}{v_y} = B_u^2 \\ B_l^3 = T_{min} \leq T_{nom} \leq T_{max} = B_u^3 \end{aligned} \tag{17}$$

where B_l^i and B_u^i are the i'th lower bound and upper bound, respectively. It should be noted that these equations are obtained assuming positive velocities. For negative values a similar procedure can be employed. Furthermore, the first two equations are valid for non-zero velocities. In the case where the velocity in one direction is zero, the bounds on that direction are ignored, and the problem is solved with the rest of the equations. In order for all the inequality constraints of (17) to be valid, the following equation should hold:

$$B_l = max(B_l^1, B_l^2, B_l^3) \leq T_{nom} \leq min(B_u^1, B_u^2, B_u^3) = B_u \tag{18}$$

Hence, using equality equations of (16) and inequality equation of (18), we can select the nominal step timing in the middle of the span and obtain other variables as well:

$$\begin{aligned} T_{nom} &= \frac{B_l + B_u}{2} \\ L_{nom} &= v_x(\frac{B_l + B_u}{2}) \\ W_{nom} &= v_y(\frac{B_l + B_u}{2}) \end{aligned} \tag{19}$$

Consistent with these nominal values, we can compute the desired DCM offsets which realize these values in the absence of disturbances. The nominal DCM offset in each direction for having nominal step length and width in nominal step duration is computed using (7).

3.2 Second stage: online foot location and timing adaptation

The second stage of our proposed algorithm deals with adapting the gait characteristics based on DCM measurement. In this stage, we are given the nominal values of the step length, step time, and DCM offset. Our goal is to find the desired values for these variables as close as possible to the nominal values, based on the current measurement of the DCM. Hence, we define an optimization problem which automatically generates the desired values at each control cycle.

By solving (2b) as a final value problem, we can write the LIPM solution in terms of the next footprint location, the step duration, and the DCM offset. Equation (6) is a nonlinear equality with respect to the step time (T). As a result, the corresponding optimization problem would be nonlinear which introduces some issues for real-time applications Herzog et al. (2015). However, further inspection on (6) reveals that by defining a new variable τ such that:

$$\tau = e^{\omega_0 T} \Longrightarrow T = \frac{1}{\omega_0} log(\tau) \tag{20}$$

We can relate (6) in a linear equality form with respect to the variables:

$$u_T - (\xi_{mea} - u_0)e^{-\omega_0 t}\tau + b = u_0 \quad , \quad 0 \leq t \leq T \tag{21}$$

The concept behind this change of variable is that rather than dividing the solution space with respect to step duration into equal parts, we divide it in a logarithmic fashion. Then, after computing τ from the optimization problem, we can use the second equation of (20) to obtain the step duration. Now

that the main equality constraint is linear, we can write the problem as a QP to yield the desired gait values as close as possible to the nominal values obtained from the first stage, and consistent with the constraints:

$$\begin{aligned}\min_{u_T,\tau,b}\ & \alpha_1\|u_T - \begin{bmatrix}L_{nom}\\ W_{nom}\end{bmatrix}\|^2 + \alpha_2|\tau-\tau_{nom}|^2 \\ & +\alpha_3\|b-\begin{bmatrix}b_{x,nom}\\ b_{y,nom}\end{bmatrix}\|^2 \\ \text{s.t.}\quad & \begin{bmatrix}L_{min}\\ W_{min}\end{bmatrix} \le u_T \le \begin{bmatrix}L_{max}\\ W_{max}\end{bmatrix} \\ & e^{\omega_0 T_{min}} \le \tau \le e^{\omega_0 T_{max}} \\ & u_T + b = (\xi_{mea}-u_0)e^{-\omega_0 t}\tau + u_0 \end{aligned} \tag{22}$$

The outputs of the optimization problem are the landing location and time of the swing foot as well as the DCM offset. It is important to note that the DCM offset should be an optimization variable because it needs to be adapted in case of large disturbances. This means, in some situations it is not possible to find a feasible set of step location and timing which realizes the desired DCM offset. Putting a very high weight for the DCM offset compared to the other terms, the optimizer always tries to find a solution such that the DCM offset is realized (if possible). If the nominal DCM offset cannot be realized perfectly, then more than one step is required to converge back to the nominal walking speed. Since we showed that the DCM offset splits state space into viable/non-viable parts, the optimization problem in (22) recovers the robot from a disturbance, if the current state of the robot is viable.

4 Swing foot trajectory adaptation

After specifying the step timing and location of the swing foot at the end of a step, the swing foot trajectory should be generated to realize the desired values. Since the next footprint and step timing can be changed at each control cycle, this procedure should be carried out in real-time. In fact, the trajectories for the swing foot should be regenerated at each control cycle to smoothly connect the desired swing foot state at the prior control cycle to the desired state at the end of step. We consider polynomials such that the trajectories are continuous at the order of acceleration to ensure smooth control policies when used in an inverse dynamics control law Herzog et al. (2016a).

The boundary conditions for the trajectories of the swing foot in the horizontal plane (x , y) can be written as:

$$\begin{aligned} X(t_{k-1}) &= X_{k-1} & X(T) &= u_T \\ \dot{X}(t_{k-1}) &= \dot{X}_{k-1} & \dot{X}(T) &= 0 \\ \ddot{X}(t_{k-1}) &= \ddot{X}_{k-1} & \ddot{X}(T) &= 0 \end{aligned} \tag{23}$$

where index k stands for the current sample time, and X can be either sagittal or lateral component of the swing foot. In order to satisfy these constraints, we employ fifth order polynomials:

$$\sum_{i=0}^{5} c_i t^i \quad , \quad t_{k-1} \le t \le T \tag{24}$$

in which c_i's are the polynomials coefficients. Using the boundary conditions of (23), the polynomials coefficients are obtained. Then, we just evaluate these polynomials for the current sample time (t_k) to obtain the desired value of the swing foot in the horizontal plane.

For the trajectory in the vertical direction, the problem is not straightforward. The reason is that the swing foot height increases to a certain value at a specified time (mid-time of the step), and then decreases to smoothly land on the ground. To generate a trajectory for the vertical component of the swing foot, we can use two fifth order polynomials for the two parts of the trajectory. For the first part, the trajectory connects the prior state to the state at the mid-time, while the second part connects the prior state to the state at the end time. However, this causes two main problems. First, change of step timing in the vicinity of the mid-time can cause a jump from the first part trajectory to the second part. Second, change of step timing in the second part generates unavoidable fluctuations in vertical direction which may cause collision of the swing foot with the ground.

Instead of two fifth order polynomials, we consider one 9th order polynomial for the whole step. The problem is to find the polynomials coefficients such that the swing foot height at the mid-time of the step is as close as possible to the desired height. Furthermore, the swing foot height during the step should be strictly positive and less than a maximum height. The polynomial coefficients are found by solving the following QP:

$$\begin{aligned}\min_{c_i}\ & \|z(T/2) - z_{des}\|^2 \\ \text{s.t.}\ & 0 \le z(t) \le z_{max} \\ & z(0)=0 \quad z(t_{k-1}) = z_{k-1} \quad z(T)=0 \\ & \dot{z}(0)=0 \quad \dot{z}(t_{k-1}) = \dot{z}_{k-1} \quad \dot{z}(T)=0 \\ & \ddot{z}(0)=0 \quad \ddot{z}(t_{k-1}) = \ddot{z}_{k-1} \quad \ddot{z}(T)=0 \end{aligned} \tag{25}$$

In this equation z is the vertical component of the swing foot. By solving this equation, the polynomial coefficients c_i's are obtained at each control cycle. Then, by evaluating the polynomial at the current time, the desired foot trajectory is obtained in real-time.

5 Whole body control

In order to obtain feasible joint torque commands from the generated trajectories in the last section, we use a hierarchical inverse dynamics controller Herzog et al. (2016a). In the employed hierarchical inverse dynamics framework, constraints and tasks are written as affine functions of joint and floating-base accelerations, actuation torques, and interaction forces and moments. In fact, these variables constitute the design variables which are optimized through a series of QPs, at each control cycle. The goal of the controller is to find the design variables that satisfy different control objectives with different priorities, while the highest priority in the hierarchy is set to ensure physical consistency. In lower priorities, various tasks with different ranks are specified, and tasks in the same priority can be weighted with respect to each other.

For all tasks, we put the equations of motion and the limits for the actuation in the highest priority. The equations of

motion can be written as:

$$M(q)\ddot{q} + N(q,\dot{q}) = S^T\tau + J_c^T\lambda \quad (26)$$

in which M is the inertia matrix, q is the vector of generalized coordinates, and N groups together the Coriolis, centrifugal and gravitational effects. S represents the joint selection matrix, τ is the vector of actuation torques, J_c is the contact jacobian, and λ is the vector of contact forces and moments. In the following, we describe lower priority tasks and constraints that can be employed in the low-level control layer.

5.1 Foot trajectory tracking

The modified trajectory for the swing foot in Section 4 should be tracked to realize the stepping task. This task can be written as:

$$J_{sw}\ddot{q} + \dot{J}_{sw}\dot{q} = \ddot{X} + K_d(\dot{X}_d - \dot{X}) + K_p(X_d - X) \quad (27)$$

in which X and X_d are the actual and reference swing foot posture vectors , and J_{sw} is the jacobian of the swing foot. Furthermore, K_p and K_d are diagonal gain matrices. It should be noted that we do not control the orientation of the swing foot because the robot has passive ankles and there is not enough DOFs to control the foot orientation. For the stance foot, the task is:

$$J_{st}\ddot{q} + \dot{J}_{st}\dot{q} = 0 \quad (28)$$

where J_{st} is the jacobian of the stance foot. This task keeps the stance foot in a stationary contact with the ground surface.

5.2 CoM height tracking

In order to track a set of desired trajectories for the CoM, we can use the following task:

$$J_{CoM}\ddot{q} + \dot{J}_{CoM}\dot{q} = \ddot{X} + K_d(\dot{X}_d - \dot{X}) + K_p(X_d - X) \quad (29)$$

where J_{CoM} specifies the CoM jacobian, and X is the vector of CoM components. Since our stepping controller does not rely on CoP modulation to steer the DCM or CoM, we do not control the CoM motion in the horizontal directions and just constrain its height to stay close to the height used in the LIP model.

5.3 Posture control

Posture control is a task in the joint space. We use this task to constrain the robot to be as much as possible in upright posture during walking. This task can be written as:

$$\ddot{q} = K_p(q_d - q) - K_d\dot{q} \quad (30)$$

In this equation, K_p and K_d are diagonal square gain matrices, with the same dimension as the actuated joints.

5.4 Force regularization

In the case of redundancy in actuation (e.g. during the double support phase), we ask the optimizer to compute contact forces as close as possible to a set of desired forces. This allows to optimally distribute the weight of the robot among the contacts while staying away from the friction cones limits.

5.5 Specification of the task hierarchy

In this subsection, we set up a hierarchy of tasks consistent with model assumptions in the stepping controller. This hierarchy is specified in TABLE 1 and is used for full humanoid simulation in Section 7. In this hierarchy, we give the highest priority to physical consistency and torque limit constraints that should be satisfied at any cost. In the second rank, we set the constraints on the stance foot to remain stationary, and on the CoM to remain on the same height as the LIPM. It should be noted that we do not control a CoM trajectory in horizontal directions. We put the swing foot control in the third rank to ensure tracking of the swing foot trajectory. The fourth rank is given to the posture control which tries to keep the robot in upright posture. Finally, the force regularization task is put in the fifth rank to regularize the ground reaction forces in the case of actuation redundancy (the double support phases at the start and end of motion).

Table 1. Hierarchy of tasks used for full humanoid simulation.

Rank	Nr. of eq/ineq constraints	Constraint/Task
1	6 eq	Newton Euler equations
	2×4 ineq	Torque limits
2	6 eq	Stance foot constraint
	1 eq	CoM height control
3	3 eq	Swing foot control
4	2×4 eq	Posture Control
5	2×6 eq	Force regularization

6 Abstract model simulation

In this section, we present simulation results obtained from applying the proposed walking controller on an abstract model of a humanoid robot. In the first scenario, we present the results obtained from simulating the LIPM. We show that the model is able to recover from more severe pushes, when our controller with step timing adjustment is used compared to the case without timing adjustment. In the second scenario, we compare our controller with the state of the art of preview control Herdt et al. (2010a) in terms of robustness against pushes.

6.1 Simulation results using the LIPM

In the first scenario, we consider the LIPM abstraction of a robot that is walking with a desired velocity. Footsteps and swing foot trajectories are computed as described in Section 3 and Section 4. During each step, the stance foot is considered as the point of contact of the LIPM. At the end of a step where the point of contact of the LIPM is changed, the foot index n is changed. By changing the foot

index, the feasible area is computed for step location, based on the current state and index of the stance foot. We apply pushes on the robot and compare the recovery capabilities of our proposed controller to the case where no step timing adjustment is employed. The robot mass is 60 Kg and the fixed CoM height is considered 80 cm, while the pelvis length is 20 cm. The limits on step length, width, and time are specified in TABLE 2. These properties approximately mimic the Sarcos humanoid robot Athena (Figure 6).

Table 2. Physical properties of the abstract model.

Value	Description	min	max
L	Step length	-50 (cm)	50 (cm)
W_{right}	Step width (right)	-10 (cm)	20 (cm)
W_{left}	Step width (left)	-20 (cm)	10 (cm)
T	Step duration	0.2 (sec)	0.8 (sec)

In this scenario, we compare our controller with one that uses fixed step durations T_{nom}. Resulting example gaits are visualized in Figure 3. The constraints on the gait properties are given in TABLE 2. It should be noted that the step location limitations are specified with respect to the stance foot. Furthermore, the values W_{right} and W_{left} are the bounds on the step width when the right foot and left foot are stance, respectively. These values should be added to l_p when the right foot is stance and subtracted from l_p when the left foot is stance to yield the limitations on the next step location (See Figure 1).

In this scenario, a velocity command (v_x=1 m/s) for forward walking is given. Based on the limitations specified in TABLE 2, the first stage of our proposed method generates the nominal step length and step duration using (19), as well as the nominal DCM offset using (7). After four steps, the robot is pushed at t=1.4 s to the right direction with a force F=325 N, during Δt = 0.1 s. We conduct two simulations to compare the results of fixed and optimized step durations. For the case (a) illustrated in Figure 3, we employ (6) for step adjustment, using DCM measurement. In this case, the step duration is not adapted and has the nominal value during the motion. As it can be observed, the robot cannot recover from the push and the DCM diverges. It should be mentioned that if the step locations were not limited, the robot could recover from the push by arbitrarily changing the location of the next step.

In the case (b) in Figure 3, we exploited the optimization procedure using (22) at each control cycle to generate the desired location and time of swing foot landing. In this case, for the first four steps where there is no disturbance, all the nominal values are realized. After applying the push in the fifth step, the robot employs a combination of step location and timing adjustment to recover from the push. In fact, the optimizer tries to find the values as close as possible to the nominal ones, while the DCM offset is given a very high weight. The result is such that after this relatively severe push, the robot makes three fast steps on the edges of the feasible area to recover from the disturbance. After the robot has recovered from the push, it continues its stepping with the desired velocity in forward direction.

In Figure 4, the obtained trajectories for each case are demonstrated. The vertical lines show the step timing which

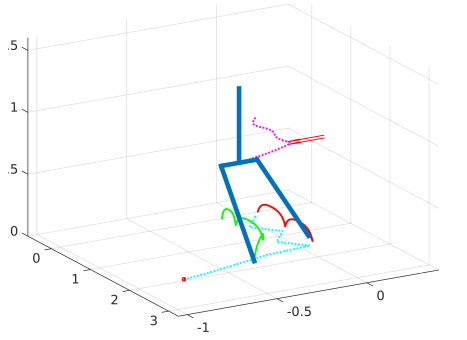

(a) without time adjustment

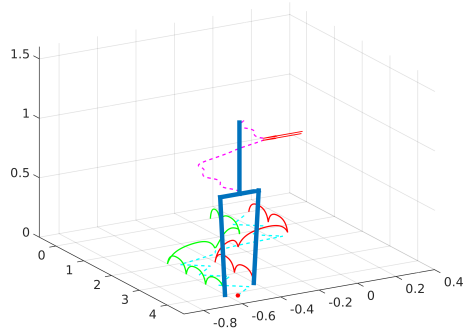

(b) with time adjustment

Figure 3. Simulation (LIPM) of walking with the nominal speed of 1 m/s (green solid: right foot, red solid: left foot, magenta dashed: CoM, Cyan dashed: DCM projection on the ground). The robot is pushed at t=1.4 s to the right direction with a force F=325 N, during Δt = 0.1 s. Step location is limited to a rectangular area and the time of stepping is limited with a minimum time (TABLE 2). case (a) (Top): The DCM diverges and the system cannot be captured without timing adjustment. Case (b) (Bottom): The system is able to recover from the push by making fast steps on the boundaries of feasible area, and continues its walking.

is fixed for the case without step timing adjustment. As it can be observed in the top figures, for the case without timing adjustment, the robot steps on the borders of feasible area to recover from the push. However, since in this case stepping can be realized just at exact times, as time goes the DCM diverges and the swing foot is not able to capture the DCM fast enough. However, in the case with timing adjustment, the algorithm adapts both next footprint and landing time based on the measured DCM. As a result, in case of a severe push, the robot steps on the borders of the feasible area very fast to recover from the push. In the bottom figures, the swing foot trajectory in vertical direction for each case is shown. As it can be observed, employing the constrained problem of (25), the swing foot trajectories in both cases are smooth and without undesired fluctuations.

6.2 Comparison with Herdt et al. (2010a)

In the second scenario, we compare the robustness of our proposed optimization procedure with time adjustment to the proposed approach in Herdt et al. (2010a). The proposed walking pattern generation approach in Herdt et al. (2010a) and variations of this technique Kajita et al. (2003); Wieber (2006); Diedam et al. (2008) are standard walking pattern generators in the literature. That is why we compare our results to this approach. The optimizer in Herdt et al.

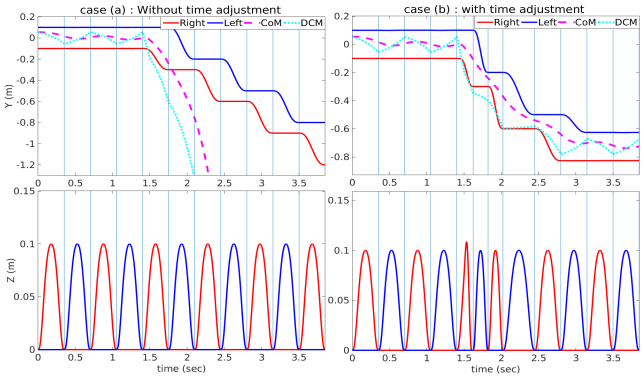

Figure 4. Comparing the trajectories for the cases with and without time adjustment. The vertical lines show the step duration. All the components of the adapted swing foot trajectory are smooth in all directions.

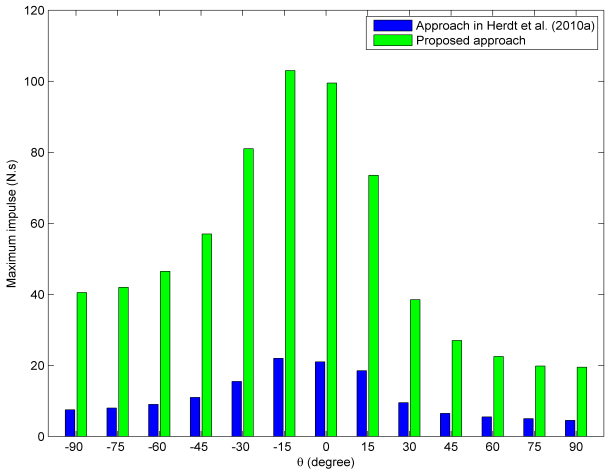

Figure 5. comparison with the approach in Herdt et al. (2010a). θ is the angle between the direction of motion and the push direction (counterclockwise). Hence, θ =0 deg corresponds to a forward push, while θ =90 deg and θ =-90 deg represent pushes to the left and right directions, respectively. For each simulation, a force during Δt =0.1 s is applied at the start of a step in which the left foot is stance. As a result, since pushes to the left direction (positive θ) impose the robot to self collision in the first step, step adjustment in this direction is more limited than the other direction. That is why the maximum push applied to the robot to the right direction (inward direction with negative θ values) is more than the left direction (outward direction with positive θ values).

(2010a) is an extension of algorithms in Kajita et al. (2003); Wieber (2006); Diedam et al. (2008) where it generates automatically both step locations and CoM trajectory for a desired walking velocity. Since in this approach the next step locations are considered as decision variables, the optimizer adapts step locations inside a feasible area while step timing is fixed. They used a horizon of N=16 time intervals with the length of T=0.1 s which results in a preview of NT=1.6 s. Solving the assembled QP for this problem with 1.6 second horizon is considerably more expensive compared to our approach in terms of computation cost.

We used the same parameters for both approaches using a LIPM with point contact and computed the maximum push that each approach can recover from in various directions (Figure 5). The value θ is the angle between the direction of motion and the push direction (counterclockwise). Hence, the negative values show the pushes to the right direction. We considered stepping with zero velocity to have symmetric results, while similar results can be obtained for different walking velocities. Therefore, the results are illustrated for -90 deg$\leq \theta \leq$ 90 deg, and for the other half symmetric results are obtained which are not shown. For each simulation, a force during Δt =0.1 s is applied at the start of a step in which the left foot is stance. It should be noted that for stepping in place with zero velocity T_{nom}=0.5 s is obtained from the first stage of our algorithm and considered for the step timing of both approaches.

As it can be observed in Figure 5, our walking controller based on a small sized QP which just adapts the swing foot landing location and time of the current step can recover from much more severe pushes compared to the approach in Herdt et al. (2010a) with a preview of several steps but without step timing adaptation. Furthermore, it can be seen that for the sideward pushes, the direction of the push affects the maximum value of the push that the robot is able to recover from. Because if the push is in the direction that with step adjustment the robot is prone to experience a self-collision (we name it outward direction, left in this case with positive θ values), the feasible area is more limited than the other direction (inward direction). Furthermore, the maximum push in the direction with $\theta = -15\,deg$ (outer corner of the rectangle of feasible area) is more than the other directions, because the feasible area for stepping in this direction is larger than the other directions.

We ran the optimizer in Herdt et al. (2010a) with minimum step timing T_{min}, and obtained as same robustness as our approach. In fact, in the case of a very severe push, both algorithms yield stepping on the boundaries of the feasible area at the minimum step timing. The difference is that in our approach stepping is done at the nominal timing as far as possible from boundaries. Then, in the case of a disturbance the step timing is adapted. However in this case, the optimizer in Herdt et al. (2010a) works with the minimum step timing as a nominal behavior which introduces many potential problems. For instance, the possibility of system failure increases. The reason is that in this case actuators will work at their maximum capability all the time and augment the risk of failure. Furthermore, the number of switching between the feet increases which makes the system more vulnerable to lose its balance due to surface unevenness. The other problem caused by stepping with the minimum step timing as a nominal behavior is a great decrease in energy efficiency. On the other hand, our algorithm will create steps at maximum speed only in case of absolute necessity which is more desirable.

7 Full humanoid simulation

In this section, we use our walking controller on a simulation of the Sarcos humanoid robot Athena in the SL simulation environment (Figure 6). Each leg of the robot has 4 active degrees of freedom with passive ankle joints and prosthetic feet. For simulating the passive ankle joints, stiff springs and dampers are used. For the low-level control, we use the hierarchical inverse dynamics described in Section 5 to generate desired joint torques for a set of desired tasks with different priorities.

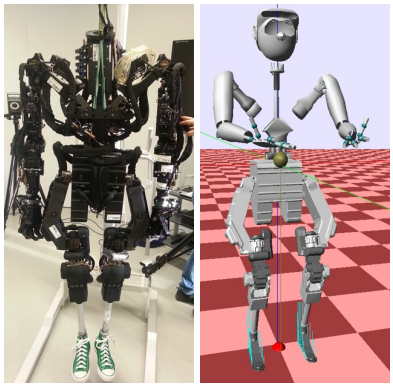

(a) real robot **(b)** simulated model

Figure 6. The Sarcos humanoid robot Athena with passive ankles and prosthetic feet

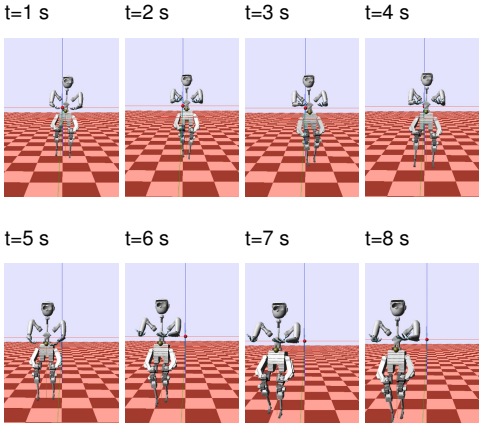

Figure 7. Athena walks forward with v_x=0.2 m/s in the SL simulation environment. The pelvis is pushed at sixth step t=3.7 s by F=200 N during Δt= 0.1 s.

Since the robot ankle joints are passive, explicitly controlling the CoM or the DCM is problematic. The reason is that unconstrained manipulation of the CoP inside the support polygon for controlling the CoM or the DCM needs large arms and upper-body motions. This is not a desired behavior during a normal walking. As a result, our controller which uses DCM measurement to adjust swing foot landing location and time is a useful tool for stabilizing this robot walking. The hierarchy of the tasks used in the hierarchical inverse dynamics is specified in TABLE 1.

In order to show the robustness of the proposed walking controller, we conduct different simulation experiments with various external disturbances (See Extension 1 for a video of full humanoid simulation on different scenarios). Since the robot has finite size feet, we use the measured CoP from the interacting forces as the current contact point u_0 in our controller. The constraints and physical properties are the same as the first scenario, except the minimum step duration which is $T_{min} = 0.3$ s. We present full body simulation in the presence of various disturbances through two scenarios. In the first scenario, the pelvis is pushed (push recovery) during stepping in different directions and the performance of the controller is investigated. In the second scenario, the stance foot is pushed during stepping such that slippage occurs (slippage recovery).

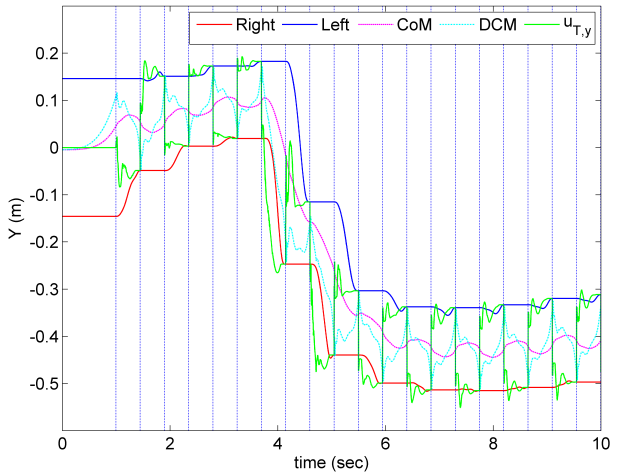

Figure 8. First push recovery experiment: The lateral trajectories during a forward walking without step timing adjustment. The desired lateral velocity is zero during this simulation. However, when the push (F=200 N, at t=3.7 s during Δt= 0.1 s which causes an impulse of 20 N.s) is exerted, the controller sacrifices lateral velocity tracking to recover the robot from the push. This push ($impulse$=20 N.s) is the maximum lateral (inward) disturbance that the robot could recover from without timing adjustment in our simulations.

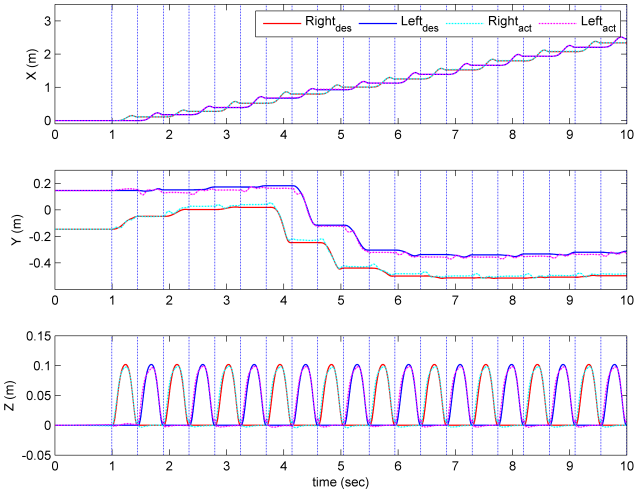

Figure 9. First push recovery experiment: The desired and actual feet trajectories during a forward walking without step timing adjustment. The low-level controller tracks the smooth feet trajectories generated by our real-time walking controller.

7.1 Push recovery

Figure 7 visualizes a forward walking simulation (v_x=0.2 m/s). In this simulation scenario, the robot pelvis is pushed to the right (inward direction) by a force F=200 N, at t=3.7 s during Δt= 0.1 s which causes an impulse of 20 N.s. To recover from the push, the robot starts stepping to the right direction. Then, once the push is rejected, the robot continues its nominal forward walking.

Figure 8 illustrates the trajectories in the lateral direction for this simulation scenario. In this figure, the updated swing foot landing point $u_{T,y}$ at each control cycle is shown. As it can be seen, the feet trajectories are adapted to realize the desired landing locations. When the push is applied, the controller sacrifices the lateral velocity tracking and adjusts

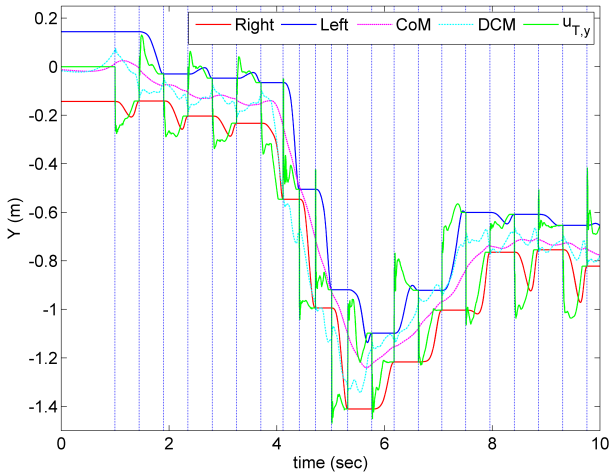

Figure 10. Second push recovery experiment: The lateral trajectories during stepping in place with both step location and timing adjustment. The desired velocity is zero during this simulation. When the push (F=390 N, at t=3.9 s during Δt= 0.3 s) is exerted, the controller adapts both step location and timing to recover from this severe lateral (inward) push. This disturbance ($impulse$=117 N.s) is the maximum lateral (inward) push that the robot could recover from with step timing adjustment in our simulations.

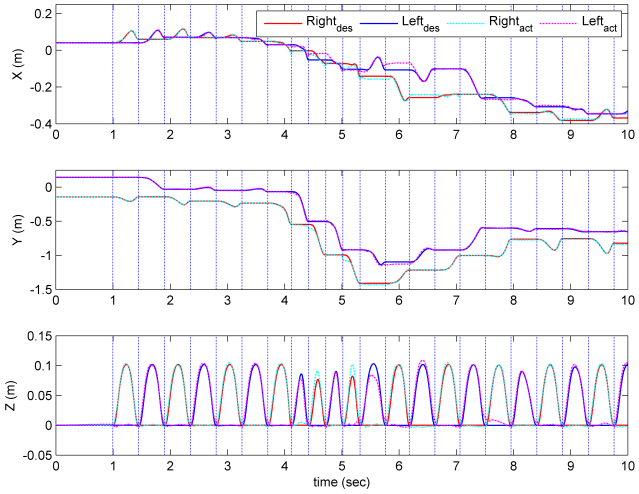

Figure 11. Second push recovery experiment: The desired and actual feet trajectories during stepping in place with both step location and timing adjustment. The low-level controller tracks the smooth feet trajectories generated by our real-time walking controller. We can see that when the step timing is adapted, the step height is adapted to satisfy the constraints specified in (25).

the gait parameters to recover the robot. Figure 9 shows the desired and actual feet trajectories. As it can be observed in this figure, the adapted trajectories of the feet are smooth, and the controller is able to track the trajectories. As it is clear in Figure 8 and Figure 9, in this case the step timing is fixed and the robot recovers from this push just by adjusting the step locations. This push ($impulse$=20 N.s) is the maximum lateral (inward) disturbance that the robot could recover from without timing adjustment in our simulations.

Figure 10 shows the significance of step timing adjustment in increasing the robustness of the gaits. In this simulation experiment, the robot steps in place and is pushed by a force F=390 N, at t=3.9 s during Δt= 0.3 s which causes an

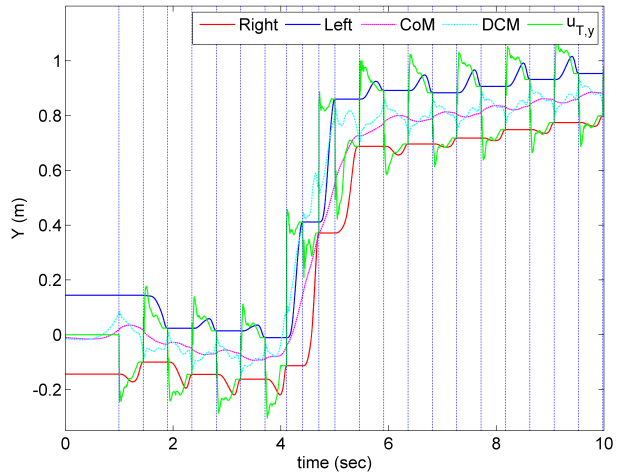

Figure 12. Third push recovery experiment: The lateral trajectories during stepping in place with both step location and timing adjustment. The desired velocity is zero during this simulation. When the push (F=290 N, at t=3.9 s during Δt= 0.3 s) is exerted, the controller adapts both step location and timing to recover from this severe lateral (outward) push.

impulse of 117 N.s. We can see in this figure that when this huge push is exerted both step location and timing are adjusted. To recover from the push, the robot takes five steps with minimum step time to the left on the boundaries of the feasible area.

This disturbance ($impulse$=117 N.s) is the maximum lateral (inward) push that the robot could recover from with step timing adjustment in our simulations. Compared to the previous scenario without step timing adjustment, the controller could recover from a push with an impulse about six times stronger. we observed similar results for LIPM simulation in Figure 5 for a push in the same direction (θ =-90 deg). This huge improvement can be explained by inspecting (3) which implies that the DCM diverges with an exponential of time. As a result, taking fast steps (decreasing the step timing) causes exponential improvement in terms of keeping the DCM from diverging. This effect is magnified, when the robot takes several steps to recover from a disturbance.

In Figure 11, the feet trajectories during this simulation experiment are shown. Again, we can see that the adapted trajectories are smooth, even in the case where step timing is adjusted. Furthermore, it can be observed that the step height is mitigated when the step duration is adapted during recovery. In fact, this shows that when the step timing is adapted, the step height is adapted as well consistent with the constraints specified in (25). As it can be seen in Figure 11, the trajectory tracking in vertical direction is degraded compared to the case without timing adjustment (Figure 9). This is due to increase in the swing foot acceleration. However, this performance for trajectory tracking in vertical direction is good enough for realizing a feasible stepping.

Figure 12 illustrates the trajectories in the case that the robot is pushed to the outward direction by a force F=290 N, at t=3.9 s during Δt= 0.3 s. This disturbance is the maximum value that the robot could recover from in the outward direction in our simulations (We observed similar behavior for LIPM simulations in Figure 5). Compared to

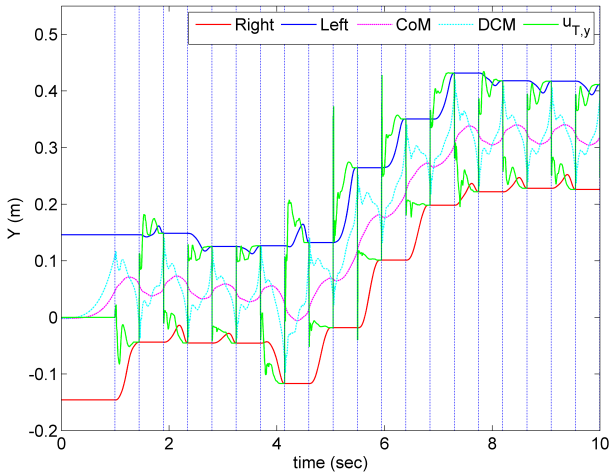

Figure 13. First slippage recovery experiment: The lateral trajectories during a forward walking without step timing adjustment. The desired lateral velocity is zero during this simulation. The stance foot is pushed laterally by F=400 N, at t=3.9 s during Δt= 0.2 s such that slippage occurs. After the push, the foot locations are adjusted to recover the robot from the push.

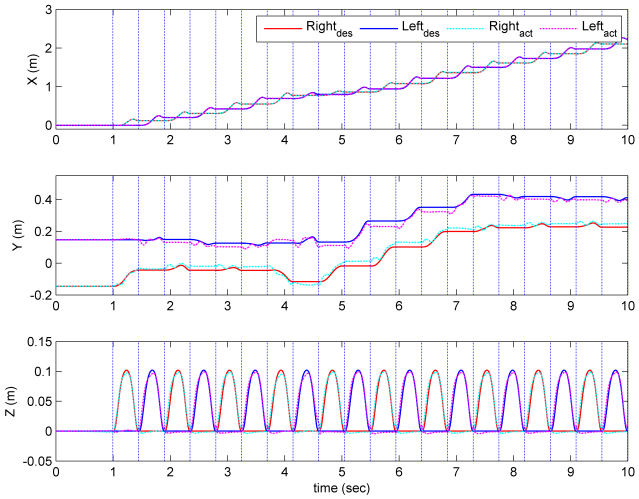

Figure 14. First slippage recovery experiment: The desired and actual feet trajectories during a forward walking without step timing adjustment. When the push is exerted at t=3.9 s, the left foot slips to the left. The right foot trajectory is then adapted to recover the robot from this disturbance.

the previous experiment, the maximum applicable push has been decreased. This is due to the fact that when the push is exerted in outward direction, to avoid the legs' self-collision, step adjustment cannot play a huge role in recovery during the step that the push is exerted. As a result, during this step the DCM diverges until in the next steps it is captured.

7.2 Slippage recovery

In the second scenario, we show the capability of our walking controller in recovering the robot from slippage. Walking controllers based on CoP modulation cannot deal with foot slippage during walking. The reason is that when the stance foot slips, the CoP is not controllable (like the case where the stance foot rotates around the edges). As a result, our walking controller which does not rely on controlling the CoP is

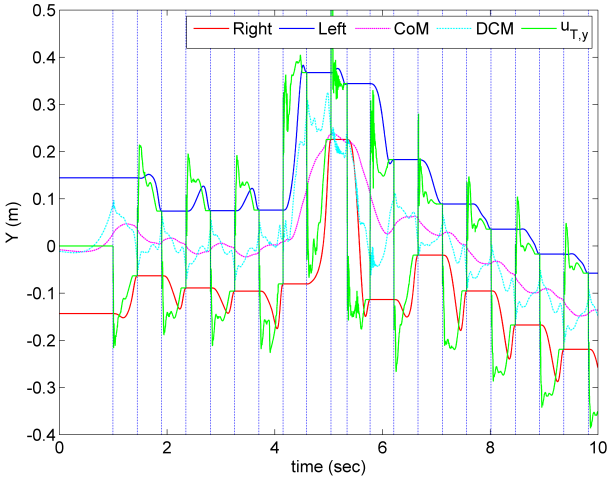

Figure 15. Second slippage recovery experiment: The lateral trajectories during stepping in place with both step location and timing adjustment. The desired velocity is zero during this simulation. The stance foot is pushed laterally by F=930 N, at t=3.9 s during Δt= 0.3 s such that slippage occurs. After the push, the foot locations are adjusted to recover the robot from the push.High frequency oscillations of the DCM trajectory is due to the huge disturbance on the stance foot. This huge disturbance causes high frequency oscillation of the passive elements in ankles.

an effective tool for recovering the robot from slippage. Recovery from foot slippage in our walking controller is done by adjusting the swing foot landing location and time.

To cause foot slippage during walking, we apply strong pushes on the stance foot such that it slips. We update the current stance foot position u_0 in our controller at each control cycle. It should be noted that the LIPM dynamics as well as the DCM definition are not valid anymore in the case of stance foot slippage. However, in this case we assume that the LIPM base remains constant during one control cycle and the definitions hold during this period. Then, we update the LIPM base (the CoP position) in the next control cycle as a new reference point for the LIPM base.

Figure 13 illustrates a forward walking simulation, while the stance foot is pushed by$F$=400 N, at t=3.9 s during Δt= 0.2 s. Slippage of the left foot in this case can be observed in the actual foot trajectory in lateral direction in Figure 14. In this case, the left foot which is stance at t=3.9 s is pushed to the left. This causes a faster DCM divergence to the right direction. Hence, the right foot which is swing steps more in the right direction to recover from this disturbance. In this case, the recovery is done without timing adjustment.

Figure 15 shows the lateral trajectories for a simulation experiment with the push F=930 N, at t=3.9 s during Δt= 0.3 s on the stance foot. In this case, the recovery is carried out by a combination of step location and timing adaptation. Again, we can see a degradation in the foot trajectory tracking in lateral direction in Figure 16. In this case, the controller exploits a combination of step timing and location adjustment to recover from this strong disturbance. Furthermore, some high frequency oscillations can be seen in Figure 15 in the DCM trajectory (and the estimated next footprint), which is due to the huge disturbance on the

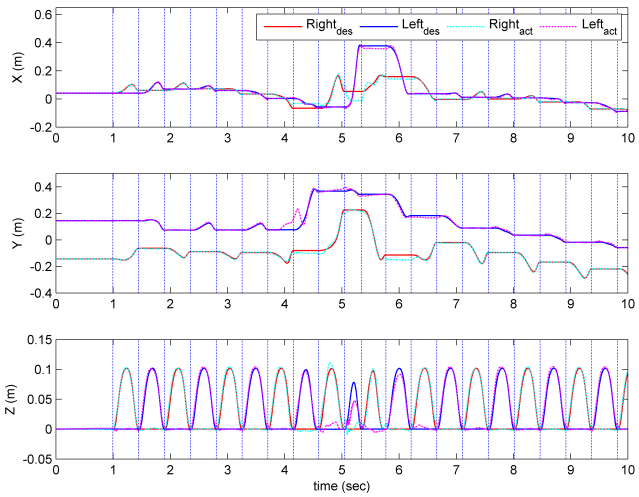

Figure 16. Second slippage recovery experiment: The desired and actual feet trajectories during stepping in place with both step location and timing adjustment. When the push is exerted at t=3.9 s, the left foot slips to the left. The next steps locations are adapted to recover the robot from the disturbance.

stance foot. This huge disturbance causes high frequency oscillations of the passive elements in ankles.

8 Discussion

In this section, we discuss the results obtained from applying our proposed walking controller on both LIPM and full model of the robot. Furthermore, we outline the limitations of the propose controller and discuss on how to circumvent them.

8.1 LIPM simulation

The following points can be deduced from the LIPM simulation results and the comparison with state of the art of preview controllers:

- *Generality* In our proposed approach, we employed step location and timing adjustment for stabilizing the stepping. In fact, without modulating the CoP at each control cycle to control the CoM or DCM, we could generate robust gaits. This suggests that our optimizer can be applied on biped robots with various structures in terms of foot geometry or actuation in ankle, i. e. with active ankle, passive ankle, or point contact foot. Moreover, as we have shown in the viability analysis, optimizing for the DCM offset over one step is enough to always keep the robot in a viable state (if such a viable state exists).
- *Linearity* A problem of including timing duration in a receding horizon approach over several steps is that the optimization problem looses linearity (as in Aftab et al. (2012); Kryczka et al. (2015)). The reason is that the time evolution of the dynamics (3) multiplies the state at the beginning of a step (ξ_0 or x_0) with an exponential of time. Both multiplication of the optimization variables and the exponential term make the main equality constraint nonlinear. In our approach, using the concept of DCM offset and the change of variable in (20), we solve a convex optimization problem with linear constraints by only looking at the next step location and timing.
- *Computational efficiency* Since in our optimization problem no horizon on future steps is considered, the size of the optimization problem drastically decreases compared to an MPC approach with several preview steps. In fact, thanks to employing the idea of DCM offset, we could split state space into viable/non-viable states. As a result, by considering the DCM offset as a decision variable in our optimization problem, we do not need to integrate the motion forward in a sufficiently large period to preserve a sufficient condition of viability Wieber et al. (2016). This results in a very small sized QP compared to common optimization-based walking controllers Kajita et al. (2003); Wieber (2006); Diedam et al. (2008); Herdt et al. (2010a).
- *Robustness* We showed that timing adjustment significantly increases robustness of the gaits. Measuring the DCM enables us to adjust the step location in the direction of an external disturbance, while step timing adaptation helps us to recover from the push very fast. Since the DCM diverges exponentially with time, timing adjustment can improve robustness exponentially. This is the key point that shows the major role of timing adjustment in recovering from external disturbances.
- *Velocity tracking* For stepping with a nominal step duration, our experiments suggested that our approach is significantly more robust than an MPC approach with several preview steps but no timing adjustment. In the case of a severe push, our optimizer and the one in Herdt et al. (2010a) sacrifice the velocity tracking to recover from the push by stepping on the boundaries. In the case of an intermediate push, our optimizer sacrifices the velocity tracking to recover from the push as soon as possible. However, since the optimizer in Herdt et al. (2010a) employs a horizon, it rejects the disturbance and also minimizes the velocity tracking error.

8.2 Full humanoid simulation

We showed the performance of our novel walking controller on a full humanoid robot without actuation in ankles in the presence of various disturbances. The following points can be deduced from obtained results:

- *Simplicity and efficiency* Our proposed stepping controller employs a simple linear dynamics (LIPM) which ignores angular momentum around the CoM and also consider fixed CoM height. This, together with introducing the idea of DCM offset and the change of variable in (20), enabled us to construct a very simple optimization problem for the walking controller. Simulations on the full humanoid model showed the great capability of our approach in rejecting disturbances despite its simplicity.
- *Viability* As we observed in results obtained from full humanoid simulation, using our controller the robot is able to recover from various disturbances by taking several steps on the edges of the reachable

area at the minimum time. In fact, the controller recovers the robot from a disturbance, if the current state is viable considering the kinematic and dynamic constraints of the robot. This is the maximum potential of a biped robot in terms of stepping to recover from external pushes. Very fast recovery from huge external disturbances with a full humanoid robot extends previous push recovery implementations by taking one step Pratt et al. (2012), or several steps Feng et al. (2016) without timing adaptation.

- *Robustness against various disturbances* The proposed controller does not rely on CoP modulation for controlling the DCM or CoM. In fact, the measured CoP and estimated DCM are employed to adapt the landing location and time of the swing foot. Therefore, it is not necessary in our control architecture that the CoP is controllable. This feature enabled us to conduct simulations with strong pushes on the pelvis and stance foot which cause rotation around the edges of the support polygon and foot slippage. In these cases the CoP is not controllable, however this does not degrade the performance of our controller. This feature should also enable the robot to walk on rough terrains, but this is left as a future work.
- *Passive ankles* A trade-off between high-inertia legs with actuated ankles and low-inertia legs with point contact feet is to use passive ankle joints together with prosthetic feet. This structure results in reduced lower leg weight and inertia, as well as a finite contact surface between the feet and the ground. However lack of actuation in ankle reduces the control authority on the CoP. We employed successfully our controller which does not rely on CoP modulation for steering the DCM or CoM to control an underactuated biped robot with passive ankle joints and prosthetic feet. Lightweight legs enabled us to have very fast reactive motion of the legs with a minimal effect on the dynamics. Moreover, having finite size feet let the CoP to move on a limited area compared to point contact feet, and also enabled the robot to perform tasks while standing (starting from standing posture).

8.3 Limitation

We discuss here the current limitations of our controller and how these could be potentially dealt with. They can be seen as open problems that will be tackled in future works.

- *Timing constraint* Constraints on step locations are explicit and depend on the kinematic and environment limitations. However, constraints on step timing are a function of maximum acceleration of the swing foot as well as the distance between the current state of the swing foot and the landing location. As a result, considering a simple constraint on step timing for the worst case decreases the performance of the controller. To circumvent this, we can employ more complex models (but linear) which take into account the swing foot dynamics Takenaka et al. (2009). Using such models, we can constrain the swing foot acceleration instead of step timing and formulate the optimization problem in a more precise fashion.
- *Angular momentum* We used the LIPM abstraction of a biped robot and proposed a walking controller which tries to employ the whole potential of the robot in terms of stepping for disturbance rejection. The other possibility that can be used to generate more robust gaits and does not depend on foot geometry or ankle actuation is regulating the angular momentum around the CoM. In order to keep the constraints linear, we could employ the LIP with flywheel model Pratt et al. (2006) and use the angular momentum as a decision variable in the optimization problem. Hence, a resulting controller would employ a combination of step location and timing adjustment together with angular momentum regulation to generate more robust gaits.
- *Walking on stepping stones* We showed that using the DCM offset concept, we do not need to consider a horizon in our walking controller to guarantee viability of the motion. However, in the case that the feasible foot locations are limited like waking over stepping stones Pratt et al. (2012), we need to add a horizon in the controller to steer the DCM motion in the direction of available contact points. This problem can be solved without adding computational burden to our walking controller by considering two steps in the first stage of our algorithm in generating nominal gait variables. Then, the nominal DCM offset is obtained such that steer the DCM motion in the direction of available contact points.
- *Gait nominal values* In the first stage of our algorithm, we used heuristics to compute gait nominal values for a given desired velocity. However, we can obtain a set of optimal gait variables in this stage to be realized for normal walking in the second stage. We can construct an optimization problem with constraints on the future steps (as we mentioned in the previous point) to obtain optimal gait nominal values in terms of some performance criteria.
- *Walking on curved paths* We formulated our walking controller for forward and sideward walking. In order to make the robot to step on a curved path, we can compute the step locations and DCM offset consistent with a desired rotation. Then, the desired swing foot and upper-body rotation trajectories can be generated consistent with the curve. Finally, by considering consistent tasks in the whole body controller, these trajectories can be realized.

9 Conclusion

In this paper, we proposed a walking controller that adapts both step location and timing in real time to generate robust gaits. This controller is based on the novel idea of DCM offset which will allow a biped to recover from disturbances as long as the current state of the robot is viable. The first stage of our walking controller computes the nominal step location and duration far from constraint boundaries for a specified walking velocity. Then, the second stage adapts these values using DCM measurement, such that the desired DCM offset is realized and the gait properties are as close as possible to the nominal values. The second stage is solved

using a quadratic program. After adapting gait variables in real time, the swing foot trajectories are regenerated using a constrained problem. Comparison with state of the art preview controllers demonstrated that the proposed approach is significantly more robust compared to the case where step adjustment without timing adjustment is employed, even when the preview controller is allowed several preview steps. Full humanoid simulations through push recovery and slippage recovery scenarios on a biped robot with passive ankles showed the robustness of our proposed controller even without control authority in the ankles.

Acknowledgements

This research was supported by the Max-Planck Society, MPI-ETH center for learning systems and the European Research Council under the European Union's Horizon 2020 research and innovation program (grant agreement No 637935).

References

Aftab Z, Robert T and Wieber PB (2012) Ankle, hip and stepping strategies for humanoid balance recovery with a single model predictive control scheme. In: *2012 12th IEEE-RAS International Conference on Humanoid Robots (Humanoids 2012)*. IEEE, pp. 159–164.

Aubin JP (1991) Viability theory. systems & control: Foundations & applications. *Birkhäuser, Boston. doi* 10(1007): 978–0.

Aubin JP and Cellina A (2012) *Differential inclusions: set-valued maps and viability theory*, volume 264. Springer Science & Business Media.

Buschmann T, Lohmeier S, Bachmayer M, Ulbrich H and Pfeiffer F (2007) A collocation method for real-time walking pattern generation. In: *2007 7th IEEE-RAS International Conference on Humanoid Robots*. IEEE, pp. 1–6.

Caron S and Kheddar A (2017) Dynamic walking over rough terrains by nonlinear predictive control of the floating-base inverted pendulum. *arXiv preprint arXiv:1703.00688* .

Caron S and Pham QC (2016) When to make a step? tackling the timing problem in multi-contact locomotion by topp-mpc. *arXiv preprint arXiv:1609.04600* .

Carpentier J, Tonneau S, Naveau M, Stasse O and Mansard N (2016) A Versatile and Efficient Pattern Generator for Generalized Legged Locomotion. In: *IEEE International Conference on Robotics and Automation (ICRA)*. Stockholm, Sweden.

Castano JA, Li Z, Zhou C, Tsagarakis N and Caldwell D (2016) Dynamic and reactive walking for humanoid robots based on foot placement control. *International Journal of Humanoid Robotics* 13(02): 1550041.

Diedam H, Dimitrov D, Wieber PB, Mombaur K and Diehl M (2008) Online walking gait generation with adaptive foot positioning through linear model predictive control. In: *2008 IEEE/RSJ International Conference on Intelligent Robots and Systems*. IEEE, pp. 1121–1126.

Englsberger J, Ott C and Albu-Schäffer A (2013) Three-dimensional bipedal walking control using divergent component of motion. In: *Intelligent Robots and Systems (IROS), 2013 IEEE/RSJ International Conference on*. IEEE, pp. 2600–2607.

Englsberger J, Ott C and Albu-Schäffer A (2015) Three-dimensional bipedal walking control based on divergent component of motion. *IEEE Transactions on Robotics* 31(2): 355–368.

Faraji S, Atkeson C, Soha P and Ijspeert A (2014a) Versatile and robust 3d walking with a simulated humanoid robot (atlas): a model predictive control approach. In: *Robotics and Automation (ICRA), IEEE International Conference on*, EPFL-CONF-196995.

Faraji S, Pouya S and Ijspeert A (2014b) Robust and agile 3d biped walking with steering capability using a footstep predictive approach. In: *Robotics Science and Systems (RSS)*, EPFL-CONF-198512.

Feng S (2016) *Online hierarchical optimization for humanoid control*. PhD Thesis, Carnegie Mellon University.

Feng S, Xinjilefu X, Atkeson CG and Kim J (2016) Robust dynamic walking using online foot step optimization. In: *Intelligent Robots and Systems (IROS), 2016 IEEE/RSJ International Conference on*. IEEE, pp. 5373–5378.

Griffin RJ, Wiedebach G, Bertrand S, Leonessa A and Pratt J (2017) Walking stabilization using step timing and location adjustment on the humanoid robot, atlas. *arXiv preprint arXiv:1703.00477* .

Harada K, Kajita S, Kaneko K and Hirukawa H (2006) An analytical method for real-time gait planning for humanoid robots. *International Journal of Humanoid Robotics* 3(01): 1–19.

Herdt A, Diedam H, Wieber PB, Dimitrov D, Mombaur K and Diehl M (2010a) Online walking motion generation with automatic footstep placement. *Advanced Robotics* 24(5-6): 719–737.

Herdt A, Perrin N and Wieber PB (2010b) Walking without thinking about it. In: *Intelligent Robots and Systems (IROS), 2010 IEEE/RSJ International Conference on*. IEEE, pp. 190–195.

Herzog A, Rotella N, Mason S, Grimminger F, Schaal S and Righetti L (2016a) Momentum control with hierarchical inverse dynamics on a torque-controlled humanoid. *Autonomous Robots* 40(3): 473–491.

Herzog A, Rotella N, Schaal S and Righetti L (2015) Trajectory generation for multi-contact momentum control. In: *Humanoid Robots (Humanoids), 2015 IEEE-RAS 15th International Conference on*. IEEE, pp. 874–880.

Herzog A, Schaal S and Righetti L (2016b) Structured contact force optimization for kino-dynamic motion generation. In: *Intelligent Robots and Systems (IROS), 2016 IEEE/RSJ International Conference on*. IEEE, pp. 2703–2710.

Hof AL (2008) The extrapolated center of mass concept suggests a simple control of balance in walking. *Human movement science* 27(1): 112–125.

Hubicki C, Grimes J, Jones M, Renjewski D, Spröwitz A, Abate A and Hurst J (2016) Atrias: Design and validation of a tether-free 3d-capable spring-mass bipedal robot. *The International Journal of Robotics Research* : 0278364916648388.

Kajita S, Kanehiro F, Kaneko K, Fujiwara K, Harada K, Yokoi K and Hirukawa H (2003) Biped walking pattern generation by using preview control of zero-moment point. In: *Robotics and Automation (ICRA), IEEE International Conference on*. IEEE, pp. 1620–1626.

Kajita S, Kanehiro F, Kaneko K, Yokoi K and Hirukawa H (2001) The 3d linear inverted pendulum mode: A simple modeling for a biped walking pattern generation. In: *Intelligent Robots*

and Systems,IEEE/RSJ International Conference on. IEEE, pp. 239–246.

Khadiv M, Herzog A, Moosavian SAA and Righetti L (2016a) Step timing adjustment: A step toward generating robust gaits. In: *Humanoid Robots (Humanoids), 2016 IEEE-RAS 16th International Conference on*. IEEE, pp. 35–42.

Khadiv M, Kleff S, Herzog A, Moosavian SAA, Schaal S and Righetti L (2016b) Stepping stabilization using a combination of dcm tracking and step adjustment. In: *Robotics and Mechatronics (ICRoM), 2016 4th RSI International Conference on, Available: https://arxiv.org/abs/1609.09822v1*.

Khadiv M, Moosavian SAA, Yousefi-Koma A, Maleki H and Sadedel M (2017) Online adaptation for humanoids walking on uncertain surfaces. *Proc IMechE Part I: Journal of Systems and Control Engineering (accepted), Available: https://arxiv.org/abs/1703.10337* .

Khadiv M, Moosavian SAA, Yousefi-Koma A, Sadedel M and Mansouri S (2015) Optimal gait planning for humanoids with 3d structure walking on slippery surfaces. *Robotica* : 1–19.

Koolen T, De Boer T, Rebula J, Goswami A and Pratt J (2012) Capturability-based analysis and control of legged locomotion, part 1: Theory and application to three simple gait models. *The International Journal of Robotics Research* 31(9): 1094–1113.

Kryczka P, Kormushev P, Tsagarakis NG and Caldwell DG (2015) Online regeneration of bipedal walking gait pattern optimizing footstep placement and timing. In: *Intelligent Robots and Systems (IROS), 2015 IEEE/RSJ International Conference on*. IEEE, pp. 3352–3357.

Kudruss M, Naveau M, Stasse O, Mansard N, Kirches C, Souères P and Mombaur K (2015) Optimal control for whole-body motion generation using center-of-mass dynamics for predefined multi-contact configurations. In: *Humanoid Robots (Humanoids), 2015 IEEE-RAS 15th International Conference on*. IEEE, pp. 684–689.

Kuo AD (2001) A simple model of bipedal walking predicts the preferred speed–step length relationship. *Journal of biomechanical engineering* 123(3): 264–269.

Kuo AD, Donelan JM and Ruina A (2005) Energetic consequences of walking like an inverted pendulum: step-to-step transitions. *Exercise and sport sciences reviews* 33(2): 88–97.

Lengagne S, Vaillant J, Yoshida E and Kheddar A (2013) Generation of whole-body optimal dynamic multi-contact motions. *The International Journal of Robotics Research* 32(9-10): 1104–1119.

Maximo MR, Ribeiro CH and Afonso RJ (2016) Mixed-integer programming for automatic walking step duration. In: *Intelligent Robots and Systems (IROS), 2016 IEEE/RSJ International Conference on*. IEEE, pp. 5399–5404.

Missura M and Behnke S (2013) Omnidirectional capture steps for bipedal walking. In: *Humanoid Robots (Humanoids), 2013 13th IEEE-RAS International Conference on*. IEEE, pp. 14–20.

Morisawa M, Harada K, Kajita S, Kaneko K, Kanehiro F, Fujiwara K, Nakaoka S and Hirukawa H (2006) A biped pattern generation allowing immediate modification of foot placement in real-time. In: *2006 6th IEEE-RAS International Conference on Humanoid Robots*. IEEE, pp. 581–586.

Morisawa M, Harada K, Kajita S, Nakaoka S, Fujiwara K, Kanehiro F, Kaneko K and Hirukawa H (2007) Experimentation of humanoid walking allowing immediate modification of foot place based on analytical solution. In: *Proceedings 2007 IEEE International Conference on Robotics and Automation*. IEEE, pp. 3989–3994.

Park IW, Kim JY, Lee J and Oh JH (2006) Online free walking trajectory generation for biped humanoid robot khr-3 (hubo). In: *Robotics and Automation, 2006. ICRA 2006. Proceedings 2006 IEEE International Conference on*. IEEE, pp. 1231–1236.

Ponton B, Herzog A, Schaal S and Righetti L (2016) A convex model of momentum dynamics for multi-contact motion generation. *arXiv preprint arXiv:1607.08644* .

Pratt J, Carff J, Drakunov S and Goswami A (2006) Capture point: A step toward humanoid push recovery. In: *2006 6th IEEE-RAS international conference on humanoid robots*. IEEE, pp. 200–207.

Pratt J, Koolen T, De Boer T, Rebula J, Cotton S, Carff J, Johnson M and Neuhaus P (2012) Capturability-based analysis and control of legged locomotion, part 2: Application to m2v2, a lower body humanoid. *The International Journal of Robotics Research* : 0278364912452762.

Takenaka T, Matsumoto T and Yoshiike T (2009) Real time motion generation and control for biped robot-1 st report: Walking gait pattern generation. In: *2009 IEEE/RSJ International Conference on Intelligent Robots and Systems*. IEEE, pp. 1084–1091.

Tassa Y, Erez T and Todorov E (2012) Synthesis and stabilization of complex behaviors through online trajectory optimization. In: *Intelligent Robots and Systems (IROS), 2012 IEEE/RSJ International Conference on*. IEEE, pp. 4906–4913.

Wieber PB (2002) On the stability of walking systems. In: *Proceedings of the international workshop on humanoid and human friendly robotics*.

Wieber PB (2006) Trajectory free linear model predictive control for stable walking in the presence of strong perturbations. In: *2006 6th IEEE-RAS International Conference on Humanoid Robots*. IEEE, pp. 137–142.

Wieber PB (2008) Viability and predictive control for safe locomotion. In: *2008 IEEE/RSJ International Conference on Intelligent Robots and Systems*. IEEE, pp. 1103–1108.

Wieber PB, Tedrake R and Kuindersma S (2016) Modeling and control of legged robots. In: *Springer Handbook of Robotics*. Springer, pp. 1203–1234.

Appendix A: Index to multimedia Extensions

See TABLE 3 for a description of the multimedia content attached to this paper.

Table 3. Index to multimedia Extensions

Extension	Media Type	Description
1	Video	A summary of full humanoid simulation on different scenarios

Appendix B: Derivation of Equation (7)

Using (4) and (5), we can write down the LIPM equations in terms of the DCM offset and the next step location :

$$u_T = (\xi_0 - u_0)e^{\omega_0 T} + u_0 - b \tag{31}$$

As it is shown in Figure 1, for a desired forward walking speed and in the absence of disturbances the DCM offsets at the start and end of a step in forward direction are the same b_x. Using this and writing (31) for forward direction give:

$$u_{T,x} = b_x e^{\omega_0 T} + u_{0,x} - b_x \tag{32}$$

The distance between two consecutive steps in forward direction is equal to the step length L. As a result:

$$b_x = \frac{L}{e^{\omega_0 T} - 1} \tag{33}$$

For a desired sideward walking, the distance between the feet is equal to $l_p + W$ or $l_p - W$ as shown in Figure 1. Using (31), we can write down the equations for the right and left foot DCM offset:

$$\begin{aligned} -(l_p - W) &= b_{y,l} e^{\omega_0 T} - b_{y,r} \\ l_p + W &= b_{y,r} e^{\omega_0 T} - b_{y,l} \end{aligned} \tag{34}$$

Solving (35) for $b_{y,r}$ and $b_{y,l}$ yields:

$$\begin{aligned} b_{y,r} &= \frac{l_p}{1 + e^{\omega_0 T}} - \frac{W}{1 - e^{\omega_0 T}} \\ b_{y,l} &= -\frac{l_p}{1 + e^{\omega_0 T}} - \frac{W}{1 - e^{\omega_0 T}} \end{aligned} \tag{35}$$

Introducing n as the index for distinguishing the left and right foot ($n = 1$ when the right foot is stance, and $n = 2$ when the left foot is stance), the DCM offset in the latteral direction can be written down as:

$$b_y = (-1)^n \frac{l_p}{1 + e^{\omega_0 T}} - \frac{W}{1 - e^{\omega_0 T}} \tag{36}$$

Appendix C: Viability in the lateral direction

Since in the lateral direction the feasible area for stepping is not symmetric with respect to the stance foot (due to self collision), the maximum allowable DCM offsets for outward and inward directions are different. It should be noted that we use outward for the direction that the legs are prone to experience a self collision, and inward for the opposite direction. We hypothesis that the maximum allowable DCM offsets in these direction are:

$$b_{y,max,out} = \frac{l_p}{1 + e^{\omega_0 T_{min}}} + \frac{W_{max} - W_{min} e^{\omega_0 T_{min}}}{1 - e^{2\omega_0 T_{min}}} \tag{37a}$$

$$b_{y,max,in} = \frac{l_p}{1 + e^{\omega_0 T_{min}}} + \frac{W_{min} - W_{max} e^{\omega_0 T_{min}}}{1 - e^{2\omega_0 T_{min}}} \tag{37b}$$

To show that these values exactly split state space into the viable and non-viable parts, we again investigate the situations where the DCM offsets are less or more than these values for both outward and inward directions. We conduct this analysis for the case where the right foot is stance, while for the other case the same results are obtained.

Outward direction

Considering a DCM offset more (less) than the value in (37a) for outward direction at the start of a step (where the right foot is stance) as:

$$\xi_{y,0} - u_{y,0} = \frac{l_p}{1 + e^{\omega_0 T_{min}}} + \frac{W_{max} - W_{min} e^{\omega_0 T_{min}}}{1 - e^{2\omega_0 T_{min}}} \pm \epsilon \tag{38}$$

the minimum feasible DCM offset at the end of this step ($b_{y,T}$) is obtained taking a step with the minimum step width (for avoiding self collision) at the minimum step time using (31):

$$\begin{aligned} b_{y,T} =& \left(\frac{l_p}{1 + e^{\omega_0 T_{min}}} + \frac{W_{max} - W_{min} e^{\omega_0 T_{min}}}{1 - e^{2\omega_0 T_{min}}} \pm \epsilon\right) e^{\omega_0 T_{min}} \\ & - (l_p + W_{min}) \end{aligned} \tag{39}$$

Using this value as the DCM offset at the start of next step, and taking a step with the maximum step width at the minimum step time yield the minimum feasible DCM offset of the next step:

$$\begin{aligned} b_{y,2T} =& \left(\frac{l_p}{1 + e^{\omega_0 T_{min}}} + \frac{W_{max} - W_{min} e^{\omega_0 T_{min}}}{1 - e^{2\omega_0 T_{min}}} \pm \epsilon\right) \\ & e^{2\omega_0 T_{min}} - (l_p + W_{min}) e^{\omega_0 T_{min}} + (l_p + W_{max}) \end{aligned} \tag{40}$$

Simplifying (40) yields:

$$b_{y,2T} = \frac{l_p}{1 + e^{\omega_0 T_{min}}} + \frac{W_{max} - W_{min} e^{\omega_0 T_{min}}}{1 - e^{2\omega_0 T_{min}}} \pm \epsilon e^{2\omega_0 T_{min}} \tag{41}$$

Comparing (38) with (41) reveals that starting from a DCM offset more than the value in (37a) (positive ϵ in (38)) and after taking two steps on the boundaries of the feasible area at the minimum time, the DCM offset increases by a factor $e^{2\omega_0 T_{min}}$ times ϵ. As a result, any DCM offset more than the value in (37a) for outward direction causes divergence. However, starting from a DCM offset less than the value in (37a) (negative ϵ in (38)), there exists one evolution (stepping on the boundaries of the feasible area at the minimum time) that keeps the DCM from diverging. Hence, we can conclude that the value in (37a) for outward direction exactly splits state space into the viable and non-viable parts.

Inward direction

Considering a DCM offset more (less) than the value in (37b) for inward direction at the start of a step (where the right foot is stance) as:

$$b_{y,max,in} = \frac{l_p}{1 + e^{\omega_0 T_{min}}} + \frac{W_{min} - W_{max} e^{\omega_0 T_{min}}}{1 - e^{2\omega_0 T_{min}}} \pm \epsilon \tag{42}$$

and taking a step with the maximum step width at the minimum possible time, the minimum feasible DCM offset at the end of the step is obtained using (31):

$$b_{y,T} = (\frac{l_p}{1+e^{\omega_0 T_{min}}} + \frac{W_{min} - W_{max}e^{\omega_0 T_{min}}}{1-e^{2\omega_0 T_{min}}} \pm \epsilon)e^{\omega_0 T_{min}} - (l_p + W_{max}) \tag{43}$$

Starting from this DCM offset and taking another step on the boundaries yield:

$$b_{y,2T} = (\frac{l_p}{1+e^{\omega_0 T_{min}}} + \frac{W_{min} - W_{max}e^{\omega_0 T_{min}}}{1-e^{2\omega_0 T_{min}}} \pm \epsilon)e^{2\omega_0 T_{min}} - (l_p + W_{max})e^{\omega_0 T_{min}} + (l_p + W_{min}) \tag{44}$$

Simplifying (44) yields:

$$b_{y,2T} = \frac{l_p}{1+e^{\omega_0 T_{min}}} + \frac{W_{min} - W_{max}e^{\omega_0 T_{min}}}{1-e^{2\omega_0 T_{min}}} \pm \epsilon e^{2\omega_0 T_{min}} \tag{45}$$

Again, comparing (42) with (45), it is clear that (37b) for inward direction exactly splits state space into the viable and non-viable parts.